

PACS numbers: 42.62.Fi; 42.55.Lt; 42.30.–d
DOI: 10.1070/QE2014v044n04ABEH015334

Stand-off detection of HMX traces by active spectral imaging with a tunable CO_2 laser

A.A. Pavlenko, E.V. Maksimenko, L.V. Chernyshova

Abstract. **Experimental results on stand-off detection of HMX traces at various surfaces using the method of active spectral imaging in the IR region are reported.**

Keywords: *explosives, spectral images, CO_2 laser.*

1. Introduction

Current studies in the area of detection of explosive materials (EMs) aimed at searching for new methods as well as at improving the existing ones are being performed all over the world. This is indicated by numerous recent publications and inventions [1 – 5].

In Russia and abroad a number of means aimed at searching for EM charges and dangerously explosive objects have been developed and now in production. These means use both direct indications (the presence of EM or its individual components) [6–9] and indirect ones (the presence of metallic and plastic details, semiconductor devices, detonating fuses, wire lines, antennas, particular shape of the case, etc.) [10].

Among all methods of EM detection the stand-off ones are worth being singled out, i.e., when the personnel performing the examination and the equipment used are located at a safe distance from the object of examination (10–100 m and more). The remoteness of detection in such methods allows not only the essential risk reduction for the personnel, civilians, instrumentation, and property in the process of investigation of fixed objects, but also the essential increase in the admissible decision time in the case of investigating moving objects, e.g., in a stream of vehicles or passengers [1, 4, 11]. The most promising methods of stand-off EM detection are the laser optical methods using the unique properties of lasers as sources of probe radiation possessing a high spectral power, monochromaticity, spatial and temporal coherence [11].

Recently a fast progress was acquired by the novel technique of remote object sensing, based on a combination of optical spectral analysis and image recognition and referred to as active spectral imaging. The published papers devoted to the application of this method to stand-off detection of traces of various chemical substances at surfaces of bodies demonstrated its high potentialities, including the identification of various EMs [12–15]. It is worth noting that there are no Russian publications on the use of this method for stand-off detection of EMs, except review papers.

In the present paper the results of studies on stand-off detection of HMX traces by means of active spectral imaging using an IR-range CO_2 laser and a commercial infrared camera with a non-cooled detector are presented.

2. Active spectral imaging method

The method consists in obtaining a multidimensional spatio-spectral image (also referred to as hyper- or multispectral image) as a result of exposing the surface of the interesting object to narrow-band monochromatic radiation from a tunable source. The tuning range of the radiation source wavelength lies within the spectral range, where the absorption bands of the substance of interest are concentrated. The role of such a source is usually played by a laser source of radiation. After the interaction of radiation with the investigated substance, the response in the form of radiation, diffusely scattered by the surface or emitted from it, which depends on the absorption coefficient of the substance, is recorded using a multielement detector. When tuning the radiation wavelength, the ratio of the energy absorbed and scattered by the object is also changed, thus producing a significant contrast between the individual details of the observed picture. The hyper- and multispectral images can be obtained both in scattered light and in the radiation, emitted by the object (Fig. 1).

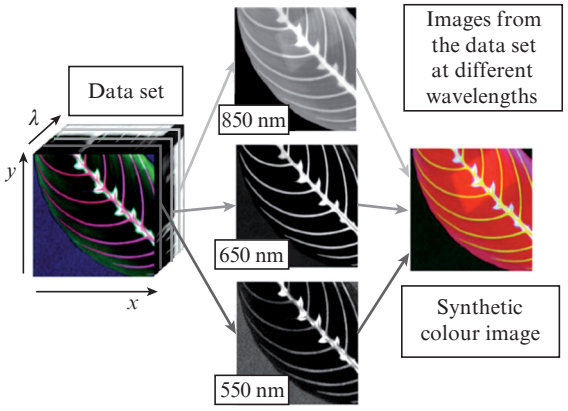

Figure 1. Example of a multispectral image [16].

A.A. Pavlenko, E.V. Maksimenko, L.V. Chernyshova Institute for Problems of Chemical and Energetic Technologies, Siberian Branch, Russian Academy of Sciences, ul Sotsialisticheskaya 1, 1659322 Biysk, Altai krai, Russia; e-mail: ipcet@mail.ru, eugene.maksimenko@yandex.ru, lvchernyshova@bk.ru

Received 28 October 2013; revision received 30 December 2013
Kvantovaya Elektronika **44** (4) 383–386 (2014)
Translated by V.L. Derbov

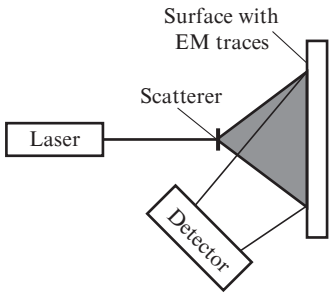

Figure 2. Scheme for illuminating the surface with the EM particles on it.

Consider the formation of a spectral image of a surface stained with EM particles using tunable laser radiation (Fig. 2). The laser radiation is scattered by the optical element and illuminates the object with EM traces on the surface, which is then observed using a multielement detector. The radiation incident on the surface is partially absorbed with the coefficient of absorption (emission) ε_{surf} and partially reflected with the coefficient of reflection r_{surf}.

According to the Kirchhoff law for a nontransparent surface, $r_{surf} = 1 - \varepsilon_{surf}$. Let us denote the emission and reflection coefficient for the EM trace by ε_{expl} and r_{expl}, respectively. The radiation recorded by the detector consists of the radiation scattered by the surface, with the total power $P_{surf} \approx r_{surf}E_{las}$, and by the EM trace, with the total power $P_{expl} \approx r_{expl}E_{las}$ (E_{las} being the laser radiation power).

The indicator that allows unambiguous identification of a substance is its IR absorption spectrum. Figure 3 presents the IR absorption spectra of some explosives, chosen from the database of the IR Fourier spectrometer 'Infralum FT-801'.

The difference in reflection (absorption) coefficients between the surface material and the EM within the entire range of the radiation wavelength tuning (IR spectra) determines the possibility of identification of the studied substance at the surface. The greater the difference, the simpler the identification, and vice versa. The multielement detector records the areas of different intensity in correspondence with the location of the EM at the surface.

First of all, the capabilities of the active spectral imaging method are determined by the spectral range of the probe radiation and the detector resolution, while the selectivity of the method depends on the possibility to distinguish between the particular IR absorption spectra of materials (absorption band positions, bandwidth, and relative intensity) by scanning the maximal spectral range, which makes it necessary to use tunable sources of probe radiation. The more spectroscopic features of the substance are assessed, the more precise is the identification.

Thus, for example, ammonium nitrate (Fig. 3a) can be detected by the fundamental absorption bands at $\lambda \simeq 3.2$, 7.2 and 12.1 μm, and TNT (Fig. 3e) by the bands at $\lambda \simeq 3.2$, 6.5,

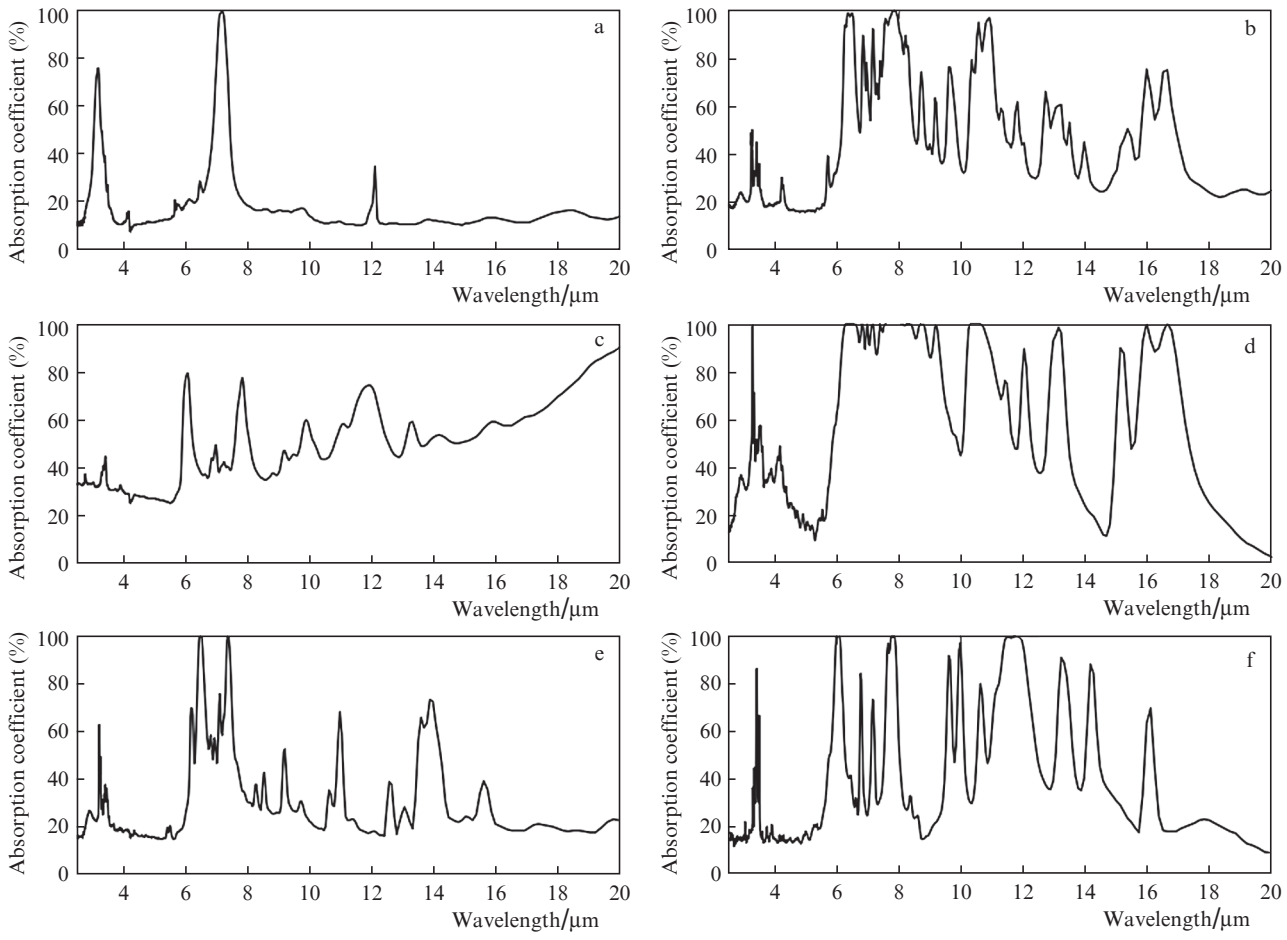

Figure 3. IR absorption spectra of some EMs: (a) ammonium nitrate, (b) RDX, (c) NG, (d) HMX, (e) TNT and (f) PETN.

7.4, 11 and 14 μm. Beside the fundamental absorption bands, other low-intensity absorption bands can be additionally used for the substance identification.

Obviously, for successful stand-off identification of EMs using a tunable CO_2 laser having a discrete set of radiation spectral lines the presence of expressed spectroscopic peculiarities (maxima and minima) in the IR spectrum of EM absorption at the laser wavelengths is necessary.

An important feature of IR spectra is that the variation in the observation angle and the object temperature uniformly affect the absorption (emission) coefficient over the entire spectral range, not giving rise to new expressed features in the absorption spectrum.

3. Experimental setup

For the study of the characteristics of the active spectral imaging method the experimental setup was developed, a schematic diagram of which is presented in Fig. 4. The LCD-5WGT wavelength-tunable CO_2 laser was chosen as a source of IR radiation. Its basic operating characteristics are presented below.

Laser radiation wavelength/μm 9.18–10.81
Radiation power (at strong lines)/W 8.0–10.5
Mode composition . . . . . 90% TEM_{00}
Polarisation. . . . . .linear
Energy divergence of laser radiation
at half-maximum level/rad. . . . . no greater than 10^{-2}
Laser radiation beam diameter
at the output mirror/mm. . . . . no greater than 1.8
Power instability of laser radiation during 30 min.
at the strongest transitions (%) . . . . . ±4.2

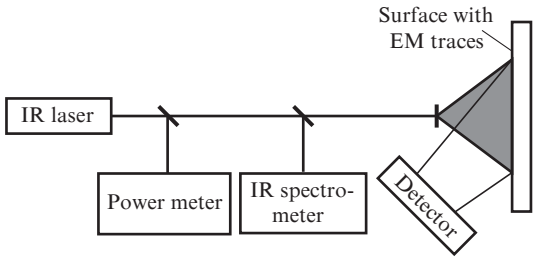

Figure 4. Scheme of the experimental setup.

The laser radiation was scattered by optical elements to illuminate the object with traces of the studied substance at the surface. The illuminated surface was observed using a thermal imaging detector. To control the radiation power and spectrum, the radiation beams were partially directed to the power meter and to the input slit of the IR spectrometer by means of beam-splitting plates. The wavelength dependences of the laser radiation power are presented in Fig. 5.

In the laser radiation spectrum the local maxima of the power are present that characterise the fundamental vibrational states of the CO_2 molecule. To obtain comparable results in recording spectral images at different wavelengths, the nonuniformity of the laser radiation power should be either hardwarily compensated by power tuning, or taken into account in further software processing.

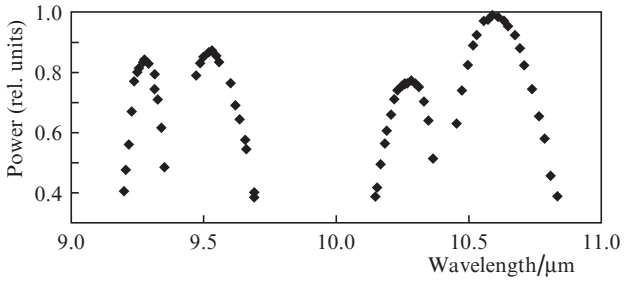

Figure 5. Wavelength dependence of the relative laser radiation power.

The laser requires forced water cooling of the radiating element and the power supply. For this aim the LAUDA WK 2200 circulatory cooler was used. The laser radiation power measurement was implemented using the Gentec EO UP19K-30H-H5-D0 power meter with the MAESTRO monitor, the basic operating characteristics of which are presented below.

Maximal power of continuous radiation/W 30
Maximal mean power during 1 min/W. 60
Effective aperture/mm 19
Spectral range/μm 0.19–20
Sensitivity/mV W^{-1} 0.65
Rise time/s 0.6

Within the laser tuning range the wavelength was measured by means of the 'Infralum FT-801' IR Fourier spectrometer whose spectral range overlaps the necessary spectral region. The operating characteristics of the IR Fourier spectrometer are presented below.

Spectral range (remote measurements)/μm 2–12
Spectral resolution/cm^{-1} 0.5, 1, 2, 4
Admissible systematic error of wavenumber
measurement/cm^{-1}. . . . . ±0.05
Admissible random error of wavenumber
measurement/cm^{-1}. . . . . ±0.02

The initial alignment of the optical system, as well as the registration of spectral IR images of the studied object, was implemented using the FLIRi60 thermal imager mounted on a stand and having the technical characteristics presented below.

Temperature range/°C . . . . . .–20 ÷ 350
Thermal sensitivity at 30 °C /°C 0.08
Accuracy. . . . . ±2 °C (±2%)
Detector type . . . . . .focal plane array (FPA) non-cooled microbolometer
IR resolution/pixels . . . . . 140×140

4. Experimental studies of samples

The study of the stand-off EM detection possibility was carried out with microscopic quantities (traces) of HMX, deposited onto different materials. Figure 6 presents the IR absorption spectrum of HMX in the tuning range of the CO_2 laser radiation. Vertical lines in the figure show the laser radiation wavelengths. The spectrum is adopted from the database of the 'Infralum FT-801' IR Fourier spectrometer .

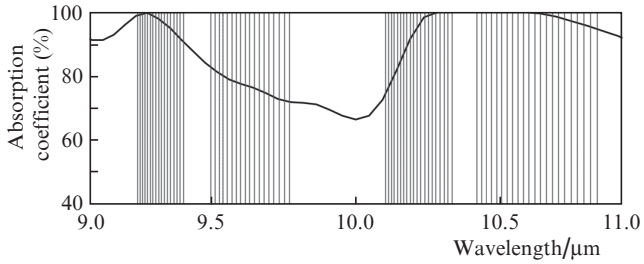

Figure 6. IR absorption spectrum of HMX.

The HMX of the VDO sort (mean particle size smaller than 50 μm, specific surface area 3000–5000 $cm^2\ g^{-1}$) was deposited onto artificial leather and paper. The scheme of HMX deposition of the surface of sample substrates is presented in Fig. 7, and the general view of the samples is shown in Fig. 8. The area of the substrate regions with HMX traces amounted to ~36 cm^2 and the specific mass of HMX did not exceed 1 mg cm^{-2}. The latter was determined by weighing on the CAS CAUS 220 analytical balance (minimum display 0.1 mg, repeatability ≤0.1 mg).

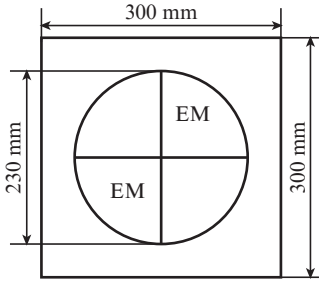

Figure 7. EM layout on the substrate.

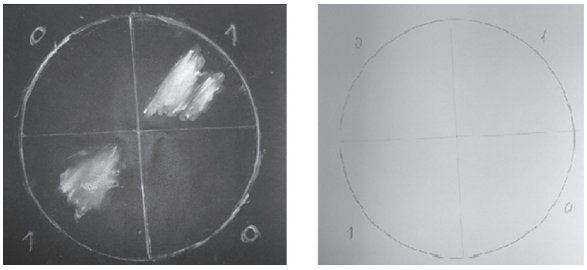

Figure 8. Samples of (a) artificial leather and (b) paper with deposited traces of HMX.

The sample substrates were placed at the distance of 1340 mm from the scattering optical element. In the studies the observation angle between the axis of the optical system and the axis of the thermal imaging device amounted to 18°. The laser radiation intensity at the surface of the object varied from 13 W m^{-2} (at the edge of the illuminated area) to 61 W m^{-2} (at the optical axis).

In real-time experiments the spectral images of HMX traces on sample substrates were obtained under the action of radiation with various wavelengths (Fig. 9).

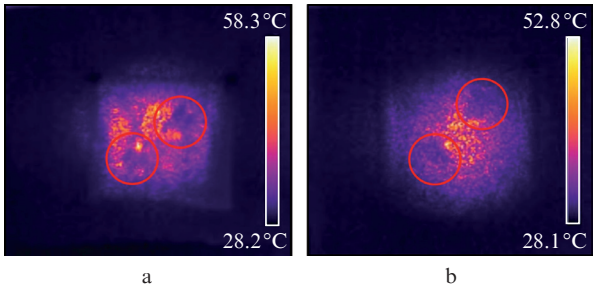

Figure 9. Thermal images of substrates made of (a) artificial leather (λ = 9.315 μm, mean temperature 33.2 °C in the area of EM deposition and 40.6 °C in the EM-free area) and of (b) paper (λ = 9.535 μm, mean temperature 32.4 °C in the area of EM deposition and 41.3 °C in the EM-free area) (b).

One can see a clear selection of the shape and position of the deposited HMX traces. The difference of the mean temperature measured using the thermal imager within the HMX deposition area and outside it attained 7.3 °C for the artificial leather substrate and 8.9 °C for the paper substrate.

5. Conclusions

The results presented in this paper demonstrate a possibility to apply the active spectral imaging method to stand-off detection of HMX traces using a tunable IR range CO_2 laser and a commercial infrared camera.

The proposed method is promising for stand-off detection of EM traces and their identification on human clothes and belongings.

References

1. *Existing and Potential Standoff Explosives Detection Techniques* (Washington DC: The National Academies Press, 2004).
2. Thiesen L., Hannum D.W., Murray D.W., Parmeter J.E. *Survey of Commercially Available Explosives Detection Technologies and Equipment 2004* (Washington: U.S. Department of Justice, 2005).
3. Caygill J.S., Davis F., Higson S.T. *Int. J. Pure Appl. Analytical Chem.*, **88**, 14 (2012).
4. Skvortsov L.A. *Kvantovaya elektronika*, **42** (1), 1 (2012) [*Quantum Electron.*, **42** (1), 1 (2012)].
5. Sil'nikov M.V., Chernyshov M.V. http://www.ormvd.ru/pubs/15189/.
6. http://www.ratec-spb.ru/index.php?catalog&devices_type=1.
7. http://www.logsys.ru/apparat/vv.htm.
8. http://www.bnti.ru/des.asp?itm=5591&tbl=02.01.01.01.
9. http://www.rapiscansystems.com/en/products/trace_detection/rapiscan_he50.
10. http://www.sds.l-3com.com/auto_explv_detect/mvt-hr.htm.
11. Munson C.A., Gottfried J.L., De Lucia F.C. *Laser-Based Detection Methods for Explosives* (Adelphy: Army Research Laboratory Weapons and Materials Research Directorate, 2007).
12. Wang Yi, Wang Y., Le H.Q. *Opt. Express*, **13** (17), 6572 (2005).
13. Phillips M.C., Hô N. *Opt. Express*, **16** (3), 1836 (2008).
14. Scharlemann E.T. *Proc. SPIE Int. Soc. Opt. Eng.*, **5154**, 126 (2003).
15. Papantonakis M.R., Kendziora C., Furstenberg R., Stepnowski S.V., Rake M., Stepnowski J., McGill R.A. *Proc. SPIE Int. Soc. Opt. Eng.*, **7304**, 730418 (2009).
16. http://www.ptgrey.com/news/pressreleases/details.asp?articleID=639